Virology 448 (2014) 265–273

Contents lists available at ScienceDirect

Virology

journal homepage: www.elsevier.com/locate/yviro

A dsRNA mycovirus, Magnaporthe oryzae chrysovirus 1-B, suppresses vegetative growth and development of the rice blast fungus ☆

Syun-ichi Urayama [a,1], Hirofumi Sakoda [a,1], Ryoko Takai [a], Yu Katoh [a], Tuong Minh Le [b], Toshiyuki Fukuhara [a], Tsutomu Arie [b], Tohru Teraoka [b], Hiromitsu Moriyama [a,*]

[a] Laboratories of Molecular and Cellular Biology, Graduate School of Agriculture, Tokyo University of Agriculture and Technology, 3-5-8 Saiwaicho, Fuchu, Tokyo 183-8509, Japan
[b] Laboratories of Plant Pathology, Graduate School of Agriculture, Tokyo University of Agriculture and Technology, 3-5-8 Saiwaicho, Fuchu, Tokyo 183-8509, Japan

ARTICLE INFO

Article history:
Received 1 August 2013
Returned to author for revisions
26 August 2013
Accepted 15 October 2013
Available online 5 November 2013

Keywords:
Mycovirus
dsRNA virus
Tentative chrysovirus
Magnaporthe oryzae
Multi-segmented mycovirus
Attenuation
Virus-induced growth inhibition

ABSTRACT

A double-stranded RNA (dsRNA) mycovirus was found in isolate S-0412-II 2a of the rice blast fungus *Magnaporthe oryzae*. Sequence analysis of the five dsRNA segments (dsRNA1 through dsRNA5) revealed that this mycovirus is closely related to Magnaporthe oryzae chrysovirus 1-A (MoCV1-A), tentatively classified as a member of the *Chrysoviridae*; therefore, it was named Magnaporthe oryzae chrysovirus 1-B (MoCV1-B). Virus particles were spherical and composed of the ORF1, ORF3 and ORF4 proteins. MoCV1-B-infected isolate S-0412-II 2a showed a more severe impaired phenotype than the MoCV1-A-infected isolate. In a virus-cured isolate, normal growth was restored, implied that MoCV1-B could be involved in this observed phenotype. An unanticipated result was the occurrence of a fungal isolate lacking dsRNA5. The nonessential dsRNA5 had higher sequence identity (96%) with dsRNA5 of MoCV1-A than with the other dsRNA segments (71–79%), indicating that dsRNA5 could be a portable genomic element between MoCV1-A and MoCV1-B.

© 2013 Elsevier Inc. All rights reserved.

Introduction

Mycoviruses have been described in many fungal species (Bao and Roossinck, 2013; Ghabrial et al., 2013; Dawe and Nuss, 2013; Hillman and Cai, 2013). Mycoviruses with dsRNA genomes are classified into four major families based on the sequence of the RNA-dependent RNA polymerase (RdRp), the *Totiviridae* (nonsegmented), *Partitiviridae* (two segments), *Chrysoviridae* (four segments) and *Reoviridae* (10–12 segments), while mycoviruses with single-stranded RNA genomes are classified into three major families, the *Hypoviridae*, *Narnaviridae* and *Barnaviridae* (King et al., 2012). Although most reported mycoviruses are apparently asymptomatic, some affect the phenotype of their fungal hosts (Anagnostakis and Day, 1979). In plant pathogenic fungi, several mycoviruses reduce the virulence of their hosts. For example, mycoviruses acting as a hypovirulence factor on their fungal host have been reported in *Cryphonectria parasitica* (Nuss, 2005), *Rosellinia necatrix* (Chiba et al., 2009; Kanematsu et al., 2004; Kondo et al., 2013) and *Fusarium graminearum* (Chu et al., 2002; Cho et al., 2013), and thus are expected to be agents for biological control of plant diseases.

Magnaporthe oryzae is a filamentous heterothallic ascomycete and the most destructive pathogen of rice worldwide. *M. oryzae* depends on its asexual spores (conidia) for disease establishment and propagation. Recently, we reported on a mycovirus, Magnaporthe oryzae chrysovirus 1 (MoCV1), found in a Vietnamese isolate of *M. oryzae* (Urayama et al., 2010). Since we report a second MoCV1 strain in this paper, the name of the first reported MoCV1 is being changed to Magnaporthe oryzae chrysovirus 1 strain A (MoCV1-A). MoCV1-A substantially impairs growth of host cells and results in altered colony morphology. To investigate potential effects of MoCV1-A gene products on host cells, a yeast heterologous expression system was constructed; overexpression of the open reading frame (ORF) 4 protein in *Saccharomyces cerevisiae* caused remarkable growth inhibition (Urayama et al., 2012). Recent studies on MoCV1-A structural proteins revealed that MoCV1-A has at least two types of viral particles, partially processed MoCV1-A and fully processed MoCV1-A (Urayama et al., 2012). Both of the viruses are isometric particles about 35 nm in diameter, with buoyant densities in CsCl ranging from 1.37 to 1.40 g cm^{-3}. The processed MoCV1-A particles are detectable not

☆The GenBank/EMBL/DDBJ accession numbers for the sequence reported in this paper.

* Corresponding author. Tel.: +81 42 367 5622; fax: +81 42 360 8830.
E-mail address: hmori714@cc.tuat.ac.jp (H. Moriyama).

[1] Syun-ichi Urayama and Hirofumi Sakoda have contributed equally to this work.

0042-6822/$ - see front matter © 2013 Elsevier Inc. All rights reserved.
http://dx.doi.org/10.1016/j.virol.2013.10.022

only in host cells but also in cell-free culture supernatants, and MoCV1-A dsRNAs can be detected within mycelia of the MoCV1-A-free isolate after co-incubation with MoCV1-A particles (Urayama et al., 2010). Phylogenetic analysis based on RdRp protein sequences showed that MoCV1-A forms a separate clade with Fusarium graminearum mycovirus-China 9 (FgV-ch9) (Darissa et al., 2011), Fusarium graminearum virus 2 (FgV2) (Yu et al., 2011), Aspergillus mycovirus 1816 (AsV1816) (Hammond et al., 2008) and Agaricus bisporus virus 1 (AbV1) (Van der Lende et al., 1996) in the family *Chrysoviridae*. While typical chrysoviruses, such as *Penicillium chrysogenum virus* (PcV) (Jiang and Ghabrial, 2004) and *Helminthosporium victoriae 145S virus* (Hv145S) (Bruenn, 2002), have four dsRNA segments, MoCV1-A, FgV-ch9 and FgV2 have five genomic dsRNA segments.

In this paper, we report a new MoCV1-A-related mycovirus, Magnaporthe oryzae chrysovirus 1 strain B (MoCV1-B), found in Vietnamese isolates of *M. oryzae* (Le et al., 2010). Five dsRNA segments ranging from 2.8 kbp to 3.5 kbp and multiform structural proteins were detected in purified MoCV1-B viral particles, which were also observed in MoCV1-A. However, a MoCV1-B-infected isolate (S-0412-II 2a) showed more severe growth defects than a MoCV1-A-infected isolate (S-0412-II 1a). During cultivation of the host fungus, we unexpectedly isolated derivative MoCV1-B, which lacks dsRNA5. The sequence of the dsRNA5 segment had extremely high similarity in MoCV1-A and MoCV1-B. We compare the effects of MoCV1-B on its host fungus and discuss the evolutionary relationship between MoCV1-A and MoCV1-B.

Results

Isolate S-0412-II 2a of M. oryzae shows a severely impaired growth phenotype

In a previous study, we found several mycovirus-infected isolates of *M. oryzae* with dsRNA genome segments ranging from 2.8 to 3.5 kbp (Urayama et al., 2010, 2012). Isolates S-0412-II 1a and S-0412-II 2a, which contained such dsRNA genomes, were picked from lesions on different rice plants in the same field. Isolate S-0412-II 2a exhibited an extremely abnormal phenotype, including loss of aerial hyphae formation and extremely reduced pigmentation, showing albino mycelia on PDA medium (Fig. 1A and C, lane 1). This phenotype was more severe than that of S-0412-II 1a, which is infected by MoCV1-A (Fig. 1B and C, lane 2) (Urayama et al., 2010). Native PAGE demonstrated that the dsRNAs of isolate S-0412-II 2a consisted of five segments, the same number as MoCV1-A (Fig. 1C). For convenience, the numbers assigned to the dsRNA genomes in S-0412-II 2a were based on sequence similarities to the MoCV1-A dsRNA genomes.

We then examined dsRNA sequence similarities among six dsRNA-harboring isolates of *M. oryzae* (Fig. 1D) by northern blotting using a subclone of the MoCV1-A dsRNA4 cDNA as probe (nt 1026–2405, AB560764). As shown in Fig. 1E, signals were detected in the dsRNAs extracted from S-0412-II 1a (lane 1, control MoCV1-A), T-0412-II 2a (lane 3) and S-0412-II 1c (lane 5), while signal was barely detected in the dsRNAs extracted from S-0412-III 1a (lane 2), T-0412-II 2b (lane 4) and S-0412-II 2a (lane 6). When we used subclones of MoCV1-A dsRNA1, 2 or 3 as probes, similar patterns of signal intensity were observed (data not shown), suggesting that the mycoviral dsRNA sequences of T-0412-II 2a and S-0412-II 1c are very similar to those of MoCV1-A, while those of isolates S-0412-III 1a, T-0412-II 1a and S-0412-II 2a are not. Thus, the mycoviral dsRNA sequences in isolate S-0412-II 2a (Fig. 1 A and C, lane 1) are different from those of MoCV1-A in isolate S-0412-II 1a (Fig. 1B and C, lane 2).

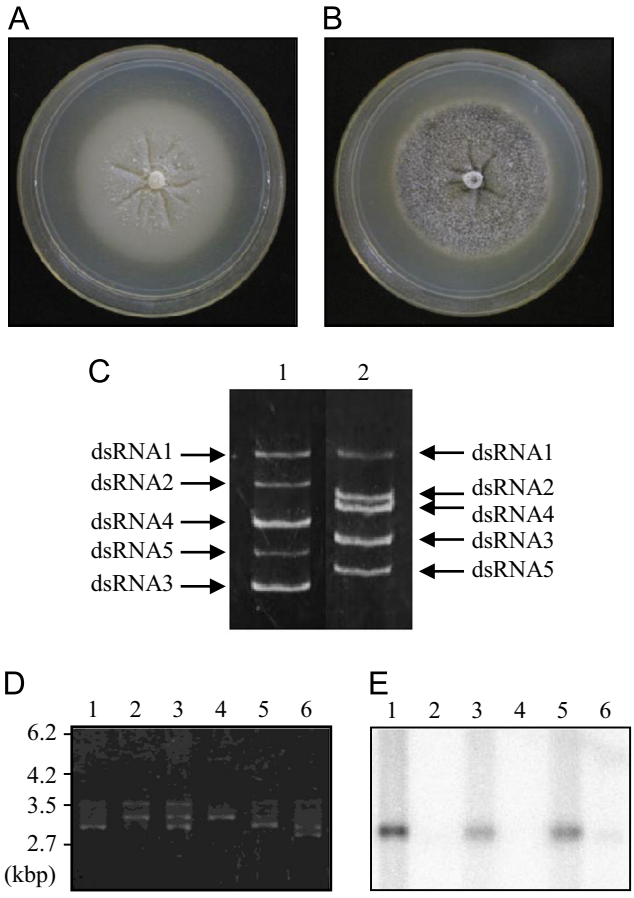

Fig. 1. Comparisons of colony morphology and dsRNAs of the S-0412-II 2a isolate and other isolates. (A, B) Comparison of colony morphology of the S-0412-II 2a isolate (MoCV1-B-infected) (A) and the S-0412-II 1a isolate (MoCV1-A-infected) (B). Both isolates were inoculated in the center of a PDA plate and incubated for 10 days at 25 °C. (C) Migration patterns of dsRNAs purified from S-0412-II 2a (MoCV1-B-infected, lane 1) and S-0412-II 1a (MoCV1-A-infected, lane 2). dsRNA was electrophoresed in 5% (w/v) polyacrylamide gels, and stained with ethidium bromide. (D, E) Agarose gel electrophoresis of dsRNAs purified from MoCV1-A-infected S-0412-II 1a (lane 1), S-0412-III 1a (lane 2), T-0412-II 2a (lane 3), T-0412-II 1a (lane 4), S-0412-II 1c (lane 5), and S-0412-II 2a (MoCV1-B-infected, lane 6), after staining with ethidium bromide (D) or the same samples after northern blotting (E). Northern blotting of purified dsRNAs extracted from *M. oryzae* Vietnam isolates using a cDNA probe derived from MoCV1-A-dsRNA4 (1026–2405 nt).

Nucleotide sequences of the five dsRNA segments in S-0412-II 2a

The complete nucleotide sequences of the five dsRNA segments in S-0412-II 2a were determined from a series of cDNA clones spanning the entire length of each dsRNA. The nucleotide sequences were significantly similar to MoCV1-A dsRNAs using the MegaBLAST algorithm of Zhang et al. (2000), and we named this mycovirus MoCV1-B. The sequences of these dsRNA segments have been deposited in GenBank/EMBL/DDBJ with accession numbers AB824667–AB824671. These five dsRNAs were named dsRNA1 to dsRNA5 based on sequence similarities to those of MoCV1-A (see Tables S1 and S2 in the Supplemental information). The genetic organization of the five dsRNAs is shown in Fig. 2A. Both the 5'- and 3'-terminal regions were conserved among the five dsRNAs of MoCV1-B and those of MoCV1-A (Fig. 2B). Comparison of nucleotide sequences of MoCV1-A and MoCV1-B revealed moderately high levels of mutual identities for dsRNA1 (79.6%), dsRNA2 (76.3%), dsRNA3 (71.4%) and dsRNA4 (72.4%), but very high levels for dsRNA 5 (96.2%) (see Table S1 in the Supplemental information). While MoCV1-A dsRNA3 and dsRNA4 carry adenine-rich regions of about 130 and 100 bp at their 3'-untranslated

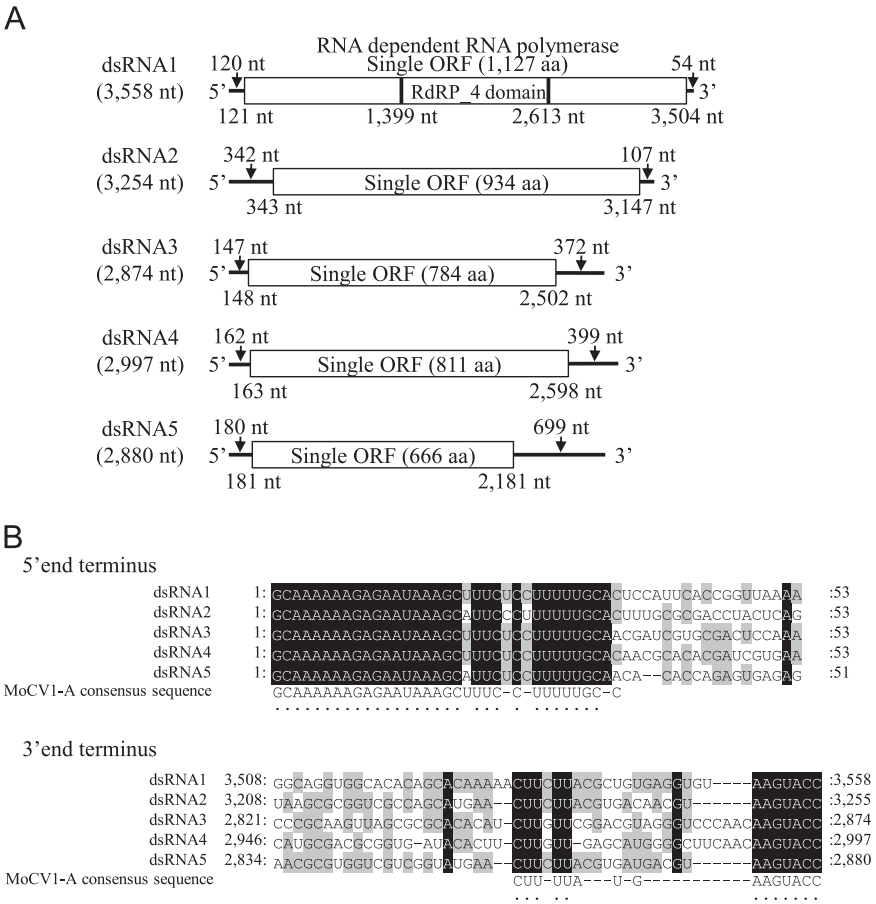

Fig. 2. Genome organization of MoCV1-B. (A) dsRNA1 comprises a 120 nt noncoding 5'-leader sequence, an ORF of 3384 nt and a 54 nt 3' noncoding sequence. dsRNA2 comprises a 342 nt noncoding 5' leader sequence, an ORF of 2805 nt and a 107 nt 3' noncoding sequence. dsRNA3 comprises a 147 nt noncoding 5' leader sequence, an ORF of 2355 nt and a 372 nt 3' noncoding sequence. dsRNA4 comprises a 162 nt noncoding 5' leader sequence, an ORF of 2436 nt and a 399 nt 3' noncoding sequence. dsRNA5 comprises a 180 nt noncoding 5' leader sequence, an ORF of 2001 nt and a 699 nt 3' noncoding sequence. (B) Multiple alignment of the 5'- and 3'-terminal regions of the coding strands of the five MoCV1-B dsRNA segments. Shading: black, 100% nucleotide identity; gray, 60–80% nucleotide identity. The MoCV1-A consensus sequence of the 5'- and 3'-terminal regions is shown under the alignment, and dots show nucleotides conserved between MoCV1-B and MoCV1-A terminal sequence.

regions (3'UTR) that were interrupted by other nucleotides (dsRNA3 (AB560763): A:93, U:29, G:8, C:4.; dsRNA4 (AB560764): A:67, U:5, G:8, C:25), no such interrupted poly(A) stretches were found in the 3'UTRs of MoCV1-B dsRNA3 (AB824669) or dsRNA4 (AB824670). The (CAA)n repeats found in the 5'UTRs of all four dsRNA segments in typical chrysoviruses were not found in MoCV1-B or MoCV1-A.

Each MoCV1-B-dsRNA encoded a single ORF. A BLAST analysis of ORF1 protein encoded by MoCV1-B-dsRNA1 revealed significant similarity to viral RdRp families (Pfam02123, RdRp_4) (Bruenn, 1993; Ghabrial, 1998). The closest relative of this domain was the RdRp encoded by MoCV1-A (92.5% identity). Phylogenetic analysis using RdRp conserved regions (Jiang and Ghabrial, 2004) showed that MoCV1-B forms a separate clade with MoCV1-A, FgV-ch9, FgV2, TcV2, AsV1816 and AbV1 in the family *Chrysoviridae* (see Figs. S1 in the Supplemental information).

A BLASTP search with predicted aa sequences of ORF2, 3, 4 and 5 revealed that these ORFs also show significant similarities to their MoCV1-A ORF counterparts: the ORF2 sequences show 80.1% identity; ORF3, 87.8% identity; ORF4, 89.4% identity; and ORF5, 97.1% identity (see Tables S2 in the Supplemental information). ORF3 also showed similarity to FgV2 ORF2 (23.3% identity, 71.5% similarity) and FgV-ch9 ORF2 (23.6% identity, 71.2% similarity), and ORF4 also showed similarity to AbV1 L3ORF (17.8% identity, 65.8% similarity), FgV2 ORF3 (15.7% identity, 59.0% similarity) and FgV-ch9 ORF3 (15.5% identity, 58.7% similarity). ORF2 and ORF5, however, did not show significant similarity to any other viral ORFs.

The alignment showed that the N-terminal sequence (aa 7–170) of MoCV1-B-ORF2 and MoCV1-A-ORF2 was less conserved, with 38.4% identity and 81.1% similarity, as was the C-terminal sequence of MoCV1-A-ORF3 (aa 661–799) and MoCV1-B-ORF3 (aa 661–784), with 66.1% identity and 91.9% similarity (see Figs. S2 and S3 in the Supplemental information). The less conserved region of ORF3 between MoCV1-A and MoCV1-B corresponds to the detached C-terminal region (approximately 200 aa) of the processed ORF3 products, designated P58 (Urayama et al., 2012).

Virus particles containing dsRNAs and multiform structural proteins

The buoyant density of purified MoCV1-B virions in CsCl was in the range of 1.37–1.40 g cm^{-3} (Fig. 3A). The five dsRNA segments were apparently packaged separately in individual virus particles; e.g., dsRNA1 was most concentrated in the fraction with buoyant density 1.40 g cm^{-3} (Fig. 3A, lane 2), dsRNA2 was in 1.39 g cm^{-3} (Fig. 3A, lane 3), while dsRNA3, dsRNA4 and dsRNA5 were in 1.38 g cm^{-3} (Fig. 3A, lane 4). After purification by CsCl density equilibrium centrifugation, fractions 2–5 (representing buoyant densities of 1.37 g cm^{-3}–1.40 g cm^{-3} in Fig. 3A) were examined via electron microscopy. Isometric virus particles with a diameter of about 35 nm were observed (Fig. 3B).

Purified virions were resolved into multiple distinct protein bands (upper region > 100 kDa; middle region 75–100 kDa; lower region < 75 kDa) after electrophoresis (Fig. 3C). Since the predicted molecular weight of ORF1 is 125 kDa, this protein might

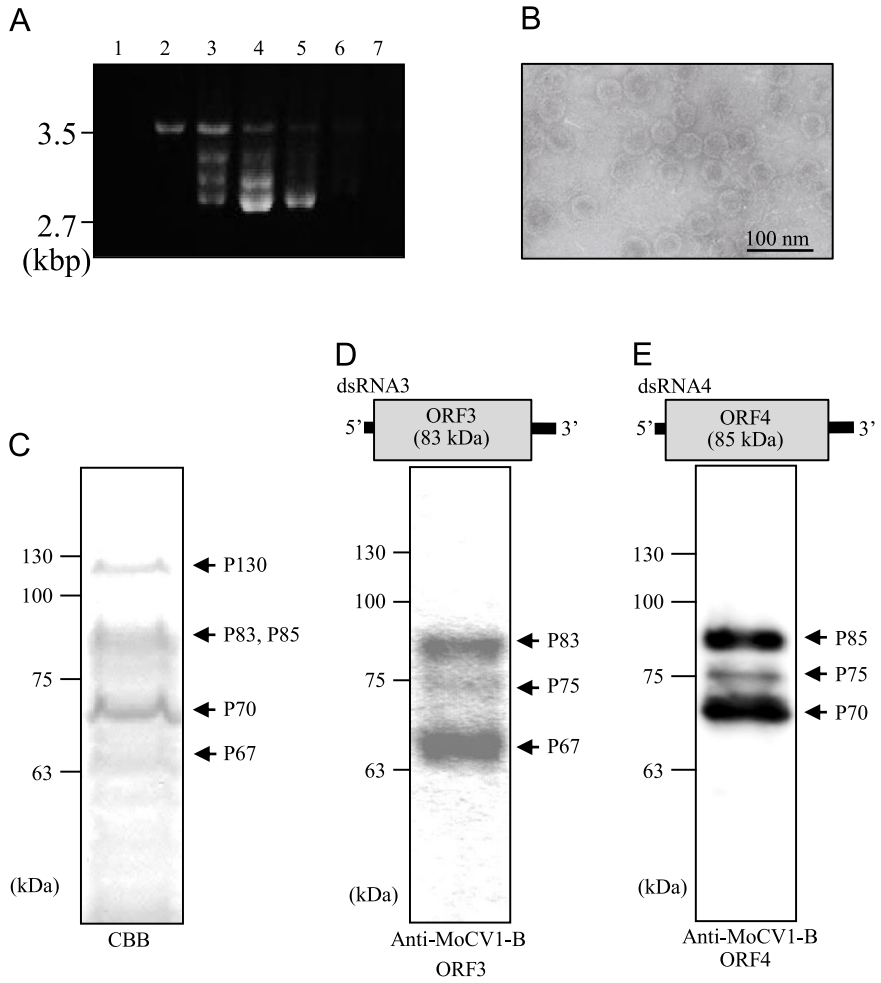

Fig. 3. Isolation of MoCV1-B particles associated with full-size ORF3 and ORF4. MoCV1-B particles were purified from mycelia of MoCV1-B-infected isolate S-0412-II 2a cultured in a fermenter for 2 days. (A) The density of each fraction was 1.40 (lane 1), 1.40 (lane 2), 1.39 (lane 3), 1.38 (lane 4), 1.38 (lane 5), 1.37 (lane 6), and 1.36 g cm^{-3} (lane 7). (B) Negative contrast electron micrograph of uranyl acetate-stained virus particles. Bar, 100 nm. Proteins of the collected virus fractions were separated by 8% SDS-PAGE (15 mA, 2 h), stained with Bio-Safe Coomassie Brilliant Blue (C) and immunoblotted with antiserum against recombinant MoCV1-B-ORF3 (D) or antiserum against recombinant MoCV1-B-ORF4 (E).

be RdRp (about 130 kDa), encoded by dsRNA1. The N-terminal sequences of the MoCV1-B structural protein bands (70 and 67 kDa) were analyzed to deduce the aa sequences of the five ORFs. The sequence of the 70-kDa band (IDQG) matched ORF4 at aa 16–19 (nt 208–219), while the N-terminal region of ORF4, aa 1–15, was absent. The sequence of the 67-kDa band (GLTLD) matched the N-terminal sequence of ORF3 at aa 2–6 (nt 151–165), suggesting that the N-terminus of ORF3 was retained, but without the methionine start codon.

Protein products of 83 and 85 kDa or MoCV1-B ORF3 and ORF4 proteins expressed in *E. coli* were consistent with the predicted molecular mass of ORF3 and ORF4, respectively (data not shown). Antiserum to the recombinant ORF3 detected an 83-kDa protein corresponding to full-size ORF3 in addition to 75- and 67-kDa proteins (Fig. 3D), while anti-ORF3 C-terminal peptide antiserum detected only an 83-kDa full-size ORF3 protein (data not shown). Anti-ORF4 antiserum detected an 85-kDa protein corresponding to full-size ORF4 as well as 75- and 70-kDa proteins (Fig. 3E). Virions purified from mycelia cultured long-term (14 days) in a fermenter contained proteolytically degraded forms of ORF3 and ORF4 proteins with sizes of 70, 65 and 58 kDa (see Fig. S4 in the Supplemental information). These proteolytic patterns were similar to those of MoCV1-A (Urayama et al., 2012). Full-sized and processed ORF3 proteins of MoCV1-B were subtly detected by anti-MoCV1-AORF3 antiserum, while full-sized and processed ORF4 proteins of MoCV1-B were distinctly detected by anti-MoCV1-AORF4 antiserum (data not shown and [Urayama et al., 2012]).

Severe suppression of vegetative growth and development by MoCV1-B

MoCV1-B-infected isolate S-0412-II 2a exhibited an abnormal phenotype, including loss of aerial hyphae formation, no subsequent conidiophore development, reduced mycelial growth and albino hyphae (Fig. 4A, left panel), whereas the MoCV1-B-free S-0412-II 2a isolate recovered normal growth (Fig. 4A, right panel). The presence or absence of MoCV1-B was confirmed by electrophoresis of the genomic dsRNAs (Fig. 4B) and by RT-PCR using primers specific for the MoCV1-B-dsRNA1 (Fig. 4C). No dsRNAs or RT-PCR product was detected from single spore clones, which showed a normal phenotype (Fig. 4B and C, lane 2). Since MoCV1-B-dsRNA1 encodes RdRp, these results indicated that single-conidium isolates had lost MoCV1-B.

The hyphae of the MoCV1-B-infected isolate were abnormally shaped, with extremely enlarged vacuoles, an increased number of branches and a lack of polarity, while healthy hyphae were observed in the MoCV1-B-free isolate (Fig. 4D). The MoCV1-B-infected isolate produced scarcely any spores relative to the

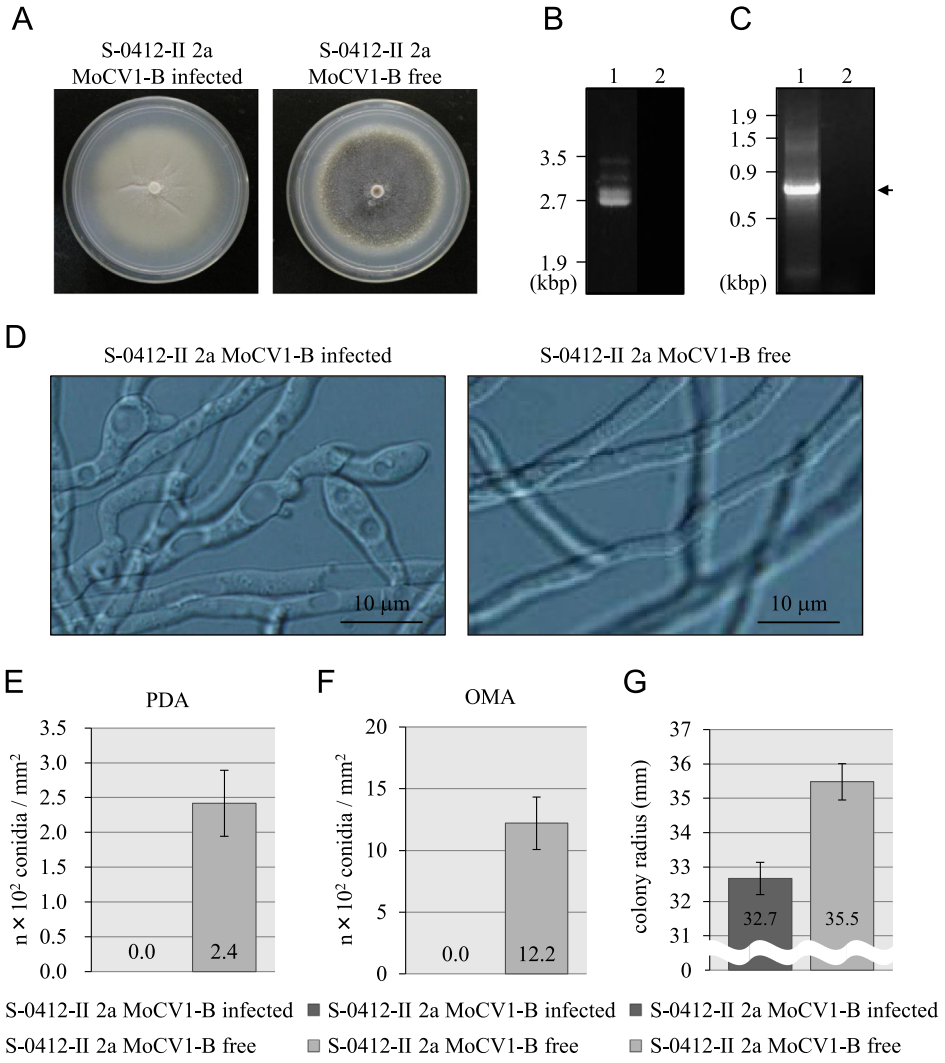

Fig. 4. Effects of MoCV1-B on morphology and selected biological traits of *M. oryzae* S-0412-II 2a. (A) Colony morphology of MoCV1-B-infected (original, left panel) and MoCV1-B-free (virus-cured, right panel) isolate S-0412-II 2a. Both isolates were inoculated in the center of a Petri dish with PDA and incubated for 14 days at 26 °C. (B) Ethidium bromide stained agarose gels after electrophoresis of dsRNAs purified from virus-infected S-0412-II 2a (lane 1) or virus-free S-0412-II 2a (lane 2). (C) Detection of MoCV1-B-dsRNA1 by RT-PCR. To confirm the presence or absence of MoCV1-B-dsRNA1, total nucleic acids were used as template for RT-PCR with MoCV1-B-dsRNA1 specific primers (5'-ACA TGG AGA AGG AGC TGG CTG A-3' and 5'-AAG TTG TCG TAA TCC AGC ATC AC-3'). Lane 1, MoCV1-B-infected S-0412-II 2a; lane 2, MoCV1-B-free S-0412-II 2a. (D) Hyphae were cultured in YG broth medium for 3 days in a fermentation reactor and observed by light microscopy using differential interference contrast optics. Hyphae of the MoCV1-B-infected isolate (left panels) and MoCV1-B-free isolate (right panels) of S-0412-II 2a are shown. Bars, 10 mm. (E, F) The mean number of spores per plate based on spore counts. Each bar represents the average of three replicates. Conidiation was assessed after growth of cultures on PDA (E) or OMA (F) at 26 °C for 2 weeks. (G) Growth analysis of *M. oryzae*. After incubation at 26 °C for 2 weeks, growth of the MoCV1-B-infected and MoCV1-B-free S-0412-II 2a on PDA was monitored by measuring colony radius. Average and standard error of measurements from four independent colonies of each strain are shown.

MoCV1-B-free isolate on OMA (Fig. 4E) or PDA (Fig. 4F). In addition to an inability to form spores, the growth rate was also reduced in the MoCV1-B-infected isolate (Fig. 4G).

dsRNA5 is dispensable for viral propagation

During subculture of the MoCV1-B-infected isolate on PDA plates, we encountered a MoCV1-B derivative that had only four dsRNA segments (Fig. 5A). Based on the migration pattern of the MoCV1-B genomic dsRNAs, the lost band was dsRNA5 (Fig. 5A, lane 2). No band could be detected by RT-PCR using dsRNA5-specific primers (Fig. 5B, lane 2). Northern blotting using a dsRNA5-specific probe also detected no signal from the isolate (Fig. 5C, lane 2). The dsRNA5-deficient MoCV1-B has been maintained in the rice blast S-0412-II 2a isolate for over 1 year through several subcultures, indicating that dsRNA5 is dispensable for MoCV1-B propagation. dsRNA5-deficient MoCV1-B was apparently accumulated in the host fungus as much as original MoCV1-B (Fig. 5A). The loss of dsRNA5 did not restore normal colony morphology (Fig. 5D and E), cell morphology, spore productivity or radial growth (data not shown) of the host fungus (the S-0412-II 2a isolate), although pigmentation was slightly restored around the inoculum plug (Fig. 5E). S-0412-II 2a isolates showed reproducible spontaneous loss of dsRNA5 during subculture.

Release of MoCV1-B from mycelium into culture supernatant

MoCV1-B-infected S-0412-II 2a isolates cultured in liquid medium were collected along with the supernatant over 2–6 weeks. MoCV1-B dsRNAs were detected after 3 weeks of culture (Fig. 6A lanes 2, 3, 4 and 5, and 6B), and reached a peak at 4–6 weeks of culture of about 250 ng dsRNA per 250 μl of culture supernatant. During prolonged culture, the amount of MoCV1-B dsRNAs that accumulated in the supernatant was reduced after 7 weeks (data not shown). In dsRNA5-deficient MoCV1-B, the other dsRNAs were also detected in the medium (Fig. 6A, lanes

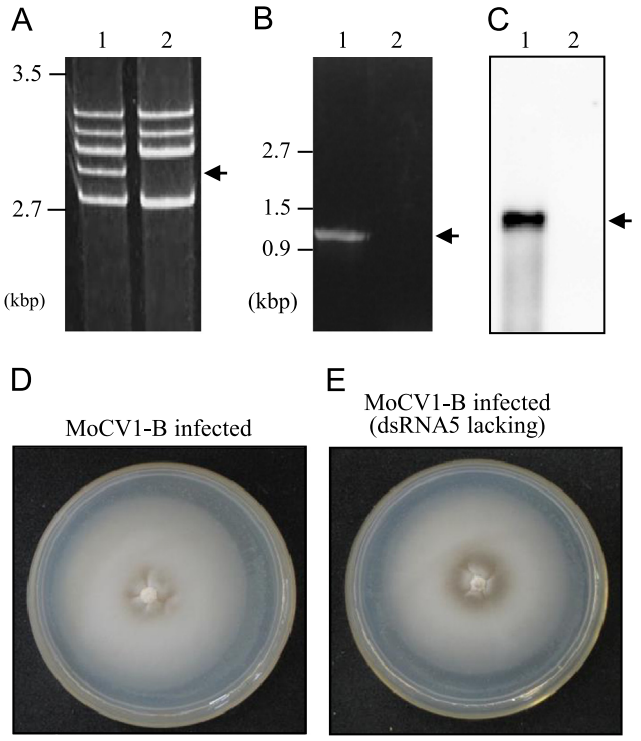

Fig. 5. Isolation of dsRNA5-deficient MoCV1-B. (A) Migration patterns of purified dsRNAs derived from MoCV1-B-infected strain (lane 1) and dsRNA5-deficient MoCV1-B-infected isolate (lane 2) of S-0412-II 2a. Total nucleic acids extracted from 50 mg fresh weight of fungal tissue were treated with S1 nuclease (TaKaRa Bio) and DNase I (TaKaRa Bio) to digest ssRNA and DNA, respectively, as previously described (Aoki et al., 2009). dsRNA was electrophoresed in 5% (w/v) polyacrylamide gels, and stained with ethidium bromide. (B) Detection of MoCV1-B-dsRNA5 by RT-PCR. To confirm the presence or absence of MoCV1-B-dsRNA5, MoCV1-B dsRNAs were used as templates for RT-PCR with MoCV1-B-dsRNA5 specific primers (5'-TGT GTG CAT GCA CCC ACA GG-3' and 5'-TGG CCA CAG TAC GCC AGT CCA CC-3'). Lane 1, MoCV1-B-infected S-0412-II 2a; lane 2, dsRNA5-deficient MoCV1-B-infected S-0412-II 2a. (C) Northern blotting analysis using cDNA derived from MoCV1-B-dsRNA5 (1945–2606 nt) as a probe. dsRNAs (0.1 mg) purified from MoCV1-B-infected S-0412-II 2a (lane 1) and dsRNA5-deficient MoCV1-B-infected S-0412-II 2a (lane 2) were blotted onto a membrane after denaturing agarose gel electrophoresis. (D, E) Comparison of colony morphology of the MoCV1-B-infected isolate (D) and dsRNA5-deficient MoCV1-B-infected isolate (E) of S-0412-II 2a. The fungal isolates were inoculated in the center of a PDA plate and incubated for 14 days at 26 °C.

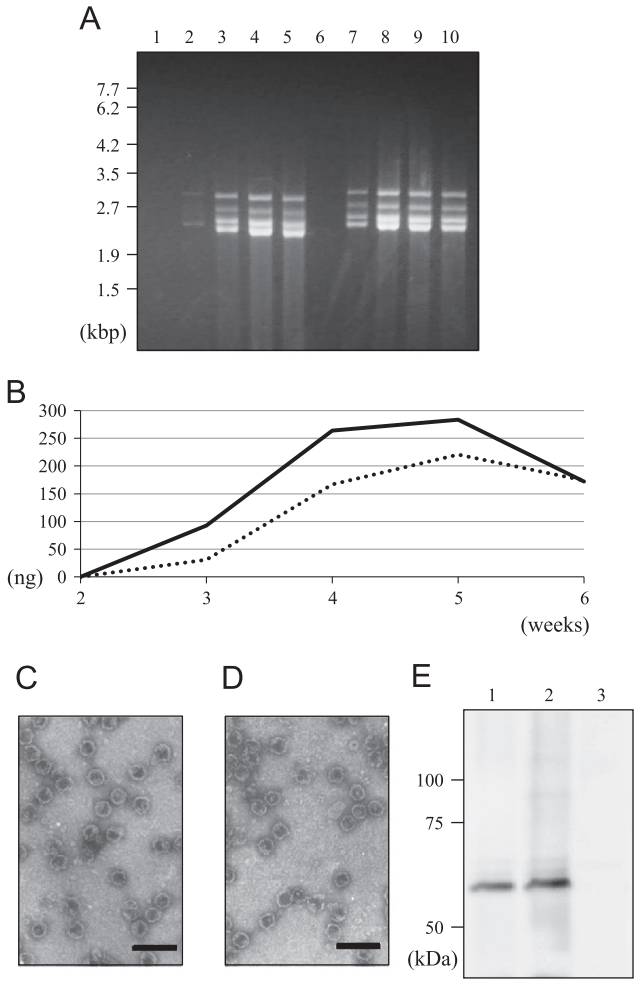

Fig. 6. Detection of MoCV1-B dsRNA genomes and virus particles in culture supernatants. (A) Agarose gel electrophoresis of total nucleic acids extracted from 250 ml culture supernatant. Supernatants were sampled every week. Lanes 1–5, MoCV1-B-infected S-0412-II 2a; lanes 6–10, dsRNA5-deficient MoCV1-B-infected S-0412-II 2a. (B) Quantification of the total intensity of the bands shown in panel A. The intensities of the bands were semi-quantified by densitometry using a CS-Analyzer ver. 3.0 (ATTO). Dotted line represents MoCV1-B-infected S-0412-II 2a, and solid line represents dsRNA5-deficient MoCV1-B-infected S-0412-II 2a. (C, D) Electron micrograph of virus-like particles released to culture supernatant. MoCV1-B-infected S-0412-II 2a (C) or dsRNA5-deficient MoCV1-B-infected S-0412-II 2a (D) were cultured for 4 weeks and the dsRNA containing supernatants were centrifuged and the resultant precipitates stained with uranyl acetate. Bar, 100 nm. (E) Western blot analysis of viral protein of MoCV1-B-infected (lane 1) and MoCV1-B-deficient (lane 2) isolate. The virus fractions were separated by SDS-PAGE and immunoblotted. Antiserum raised against purified MoCV1-B particles was used for immunoblotting. The control was the sample derived from the MoCV1-B-free isolate of S-0412-II 2a (lane 3).

7–10, and 6B). After culturing for 6 weeks, isometric virus particles (ca. 35 nm) were observed by electron microscopy in samples precipitated by ultracentrifuge of the culture supernatant of MoCV1-B-infected S-0412-II 2a (Fig. 6C), but not MoCV1-B-free S-0412-II 2a (data not shown). MoCV1-B viral proteins with a size of 58 kDa were also detected with anti-MoCV1-B antiserum (Fig. 6E, lane 1). Isometric virus particles of dsRNA5-deficient MoCV1-B were also observed (Fig. 6D) and these viral proteins with a size of 58 kDa were also detected by anti-MoCV1-B antiserum (Fig. 6E, lane 2), suggesting that dsRNA5 is not essential for release of MoCV1-B particles from host cells or for stability of the particles in the culture medium.

Discussion

We isolated and characterized a dsRNA mycovirus designated MoCV1-B, which was closely related to MoCV1-A. MoCV1-B shared common traits with MoCV1-A, such as proteolytically degraded viral proteins in host fungi cultured for a long period in liquid medium (Fig. S4 and Urayama et al., 2012), and presence of the degraded virus particles in liquid medium after prolonged culture (Fig. 6 and Urayama et al., 2010).

Analysis of the proteins of purified MoCV1-B particles indicated that they contain at least three viral proteins, including the ORF1, ORF3 and ORF4 proteins. The major structural proteins encoded by multiple segments were intriguing because such an example is rare for a mycovirus. The major structural proteins of Botrytis porri RNA virus 1 and members of the family Quadriviridae are encoded by two dsRNA segments (Wu et al., 2012; Lin et al., 2012, 2013). RdRp of these two viruses seems to be barely detectable in purified virus particles, although a distinct band of full-sized ORF1 protein encoding RdRp was detected from virus particles of MoCV1-A and MoCV1-B. Since the N-terminus of ORF1 would be blocked (Urayama et al., 2012), the blocked ORF1 would be tolerant to photolytic degradation, and thereby be suitable as a component of the viral structural protein.

The 58-kDa MoCV1-B protein purified from mycelia was a proteolytic derivative of full-size ORF3 protein. The aa sequences of these proteolytically cleaved 58-kDa proteins were highly conserved between MoCV1-B-ORF3 (M1 to Y592) and MoCV1-A-ORF3 (M1 to Q592) (93.6% identity). On the other hand, the proteolytically cleaved C-terminal region was less conserved than the N-terminus; the sequence of predicted processing regions of MoCV1-B-ORF3 (E593 to L784) and MoCV1-A-ORF3 (E593 to L799) showed 69.8% identity and 93.2% similarity. Degraded 58-kDa proteins could still be components of the particle structure. In MoCV1-A, degraded 58-kDa proteins are also found in intact virus particles; therefore, as postulated for MoCV1-A (Urayama et al., 2012), MoCV1-B particles might exist in at least two forms. This highly mutated region might be responsible for the specificity of virion structure or virulence on host fungi. N-terminal analysis of the 70-kDa protein suggested that it is similarly a C-terminal degraded derivative of full-size ORF4 protein. However, the predicted aa sequence of the ORF4 C-terminal region was relatively conserved between MoCV1-B-ORF4 (aa 676–811) and MoCV1-A-ORF4 (aa 676–812) (82.4% identity) (see Figs. S5 in the Supplemental information). The degradation of mycoviral structural proteins has also been reported by Lin et al. ; in this case, two *Rosellinia necatrix quadrivirus 1* strains differed in the degree of susceptibility of two major capsid proteins to proteolytic degradation (Lin et al., 2013).

Comparison of the entire sequences of the five dsRNA segments revealed that the 5'- and 3'-terminal sequences of MoCV1-B and MoCV1-A are almost identical (Fig. 2B and [Urayama et al., 2012]). The dsRNA5 segments were especially highly conserved between the two viruses (nucleic acid, 96% identity; aa, 97% identity), compared to the other dsRNA segments (see Tables S1 and S2 in the Supplemental information), suggesting that dsRNA5 was recently transmitted from one virus to another; in other words, dsRNA5 might be a portable genetic element between MoCV1-A and MoCV1-B. Because their hosts, S-0412-II 2a (MoCV1-B-infected) and S-0412-II 1a (MoCV1-A-infected), were isolated from the same field, there was an opportunity for the two MoCVs to coexist, and for dsRNA5 to be packaged into the capsid proteins, switching virions during hyphal fusion (anastomosis) of the host fungus. The occurrence of hyphal fusion between these two isolates was confirmed in preliminary experiments. It will be of interest to know whether dsRNA5 shows variation in nature.

In this study, dsRNA5 was dispensable for viral propagation, at least during in vitro culture, and the loss of dsRNA5 did not result in any apparent phenotypic change to the host *M. oryzae*, nor did it affect viral replication. There is a precedent for a dsRNA mycovirus having lost a genome segment. The initial isolates of the reovirus of *Rosellinia necatrix* were found to have 12 segments, but isolates with only 11 segments were later found, indicating that one of the segments, segment 8, is not required for virus replication or maintenance (Kanematsu et al., 2004). It is possible that dsRNA5 is necessary for stable propagation of MoCV1-B in the field, or that dsRNA5 is a satellite RNA of MoCV1-B. In contrast to the packaging system of Rosellinia necatrix reovirus, the particles of which contain 11 or 12 dsRNA segments, each dsRNA segment seems to be packaged into a virus particle of MoCV1-A or MoCV1-B (Urayama et al., 2010), suggesting that the observed dsRNA-loss events might be responsible for distinct packaging systems. Recently, it has been reported that Raphanus sativus chrysovirus 1, phylogenetically classified in the *Chrysoviridae*, has only three dsRNA segments (Li et al., 2013), although most chrysoviruses have four. MoCV1-B, MoCV1-A, FgV-ch9 and FgV2 have five dsRNA segments, although TcV2 has four dsRNAs (Herrero and Zabalgogeazcoa, 2011). The segment numbers of AsV1816 and AbV1 have not yet been determined (Hammond et al., 2008; Van der Lende et al., 1996). These data suggest that chrysovirus-related viruses might harbor a variable number of dsRNA genome segments.

The phenotypic changes caused by MoCV1-B were more severe than those caused by MoCV1-A, suggesting that MoCV1-B is more virulent than MoCV1-A against the host fungus, *M. oryzae*. Reciprocal virus transmission experiments between S-0412-II 1a (MoCV1-A-infected or -free) and S-0412-II 2a (MoCV1-B-infected or -free) therefore need to be undertaken to demonstrate the severe phenotypes caused by MoCV1-B. Even if host factors are involved in the development of severe phenotypes, the loss of conidiophores and pigmentation is still an important phenotype, because such a phenotype is thought to be associated with reduced or abolished virulence of rice blast fungus. Indeed, the melanin biosynthetic pathway is a specific target of some commercial fungicides. Elucidation of the molecular mechanism behind the MoCV1-B effects may lead to the discovery of novel biocontrol and antifungal proteins.

The isometric dsRNA mycoviruses are classified into four major families, the *Totiviridae*, *Partitiviridae*, *Chrysoviridae* and *Reoviridae*. Phylogenetic analysis revealed that MoCV1-A and MoCV1-B are related to Chrysoviruses, but form a sister clade with AbV1, FgV2, FgV-ch9, TcV2 and AsV1816. MoCV1-A and MoCV1-B showed unique characteristics compared with mycoviruses assigned to these four viral families, such as the number of dsRNA segments (five segments) and the transient presence of virus particles in liquid medium. MoCV1-A and MoCV1-B are thus members of a new group of dsRNA mycoviruses in the *Chrysoviridae*.

Materials and methods

Fungal strains and culture methods

All isolates of *M. oryzae* used in this paper were obtained from symptomatic rice leaves sampled in Vietnam (Le et al., 2010). The MoCV1-B-infected S-0412-II 2a isolate (the original isolate) and a MoCV1-B-free S-0412-II 2a isolate (MoCV1-B-cured isolate) of *M. oryzae* were grown on potato dextrose agar (PDA) (Yang et al., 2009) at 26 °C. Isolates were also cultured in 0.5% yeast extract and 2% glucose liquid broth (YG broth) in flasks (60 strokes per min, 26 °C) or a fermentation reactor (2.5 L, 27 °C, ABLE Biott, Tokyo, Japan) as described (Urayama et al., 2012).

cDNA cloning

Purification of dsRNAs from mycelia or purified MoCV1-B particles followed published procedures (Aoki et al., 2009; Urayama et al., 2010). The five dsRNA segments isolated from *M. oryzae* isolate S-0412-II 2a were used as templates for cDNA synthesis, and a series of overlapping cDNA clones was obtained. These cDNA clones were confirmed to be derived from the five dsRNA segments of isolate S-0412-II 2a by northern blotting and RT-PCR (data not shown). The 5'- and 3'-terminal sequences of all five dsRNAs were respectively determined using 5' and 3' rapid amplification of cDNA ends (Frohman et al., 1988).

Phylogenetic and sequence analysis

Multiple alignments based on the deduced amino acid (aa) sequences of the putative RdRp gene of MoCV1-B, PcV and MoCV1-related viruses were obtained by a series of pairwise alignments using ClustalX 2.0 (Larkin et al., 2007; Thompson et al., 1997) and MEGA5 software (Tamura et al., 2011). Phylogenetic analysis under the maximum likelihood framework was conducted using PhyML 3.1 (Guindon et al., 2010) with the best-fit models of aa substitution selected by ProtTest2.4 (Abascal et al., 2005), as judged by the Akaike information criterion (Posada and Buckley, 2004). The models employed were LG+I+G+F. Numbers

on branches indicate bootstrap support values for 1000 replicates. Sequence analysis was performed using Genetyx software version 9.1.0 (Genetyx Corp., Tokyo, Japan).

Protein sequencing

For sequencing the N-terminal peptides of MoCV1-B P70 and P67, purified MoCV1-B proteins were separated by 8% SDS-PAGE and blotted to a Clear Blot P PVDF membrane (ATTO, Tokyo, Japan). After staining with Bio-Safe Coomassie Brilliant Blue (Bio-Rad, Hercules, CA, USA), the proteins were cut out of the membrane and sequenced by automated Edman degradation using an LC-10Avp system (Shimadzu Techno-Research, Kyoto, Japan).

Purification of virus particles from mycelia

Fresh mycelia of the MoCV1-B-infected S-0412-II 2a isolate, which had been cultured for 2 days, were homogenized in a mixer with 10 volumes of 0.1 M sodium phosphate buffer (pH 7.4) containing 0.2 M KCl (buffer A) at 4 °C, in order to purify full-sized virus particles, which were composed of 84 kDa ORF3 and 85 kDa ORF4, based on our approach with MoCV1-A (Urayama et al., 2012). The homogenate was centrifuged at 22,000*g* for 15 min. The supernatant was ultracentrifuged at 148,400*g* for 1 h in a Hitachi CP80WX P45AT rotor, and the resultant precipitate was suspended in buffer A at 4 °C. The suspension was applied to sucrose density gradients (100–400 mg ml^{-1}) in buffer A and centrifuged at 112,700*g* for 2.5 h. The dsRNA-containing fractions were combined and diluted with buffer A. The solution was ultracentrifuged at 148,400*g* for 1 h and the pellets were resuspended in the same buffer. Isolated viral particles were stained with 2% uranyl acetate and observed using an H7100 transmission electron microscope (Hitachi). Proteins of the purified viral preparation were analyzed by 8% SDS-PAGE with 25 mM Tris/glycine and 0.1% SDS at 15 mA for 2 h. After electrophoresis, the gels were stained with Bio-Safe Coomassie Brilliant Blue. In order to obtain anti-MoCV1-B antiserum, rabbits were immunized with 1.35 mg of the gradient-purified MoCV1-B particles.

Expression of ORF3 and ORF4 proteins in Escherichia coli

Recombinant MoCV1-B ORF3 and ORF4 proteins were expressed in *E. coli* using a pET expression system and purified by nickel-agarose chromatography (Urayama et al., 2012).

Western blotting

Virus samples were separated by 8% SDS-PAGE in 25 mM Tris-glycine and 0.1% SDS at 15 mA for 2 h. Proteins were electrotransferred to PVDF membranes using an AE-6677 semidry electrophoretic transfer system (ATTO). Membranes were treated with blocking buffer (5% skim milk, 0.2% Tween 20 in PBS) and then sequentially with primary and secondary antibodies diluted in Can Get Signal solution (Toyobo, Osaka, Japan). Rabbit antiserum raised against purified MoCV1-B particles and rabbit antiserum raised against recombinant MoCV1-B-ORF3 or MoCV1-B-ORF4 were used to detect MoCV1-B viral proteins. After membranes were washed, the blots were developed with ECL Plus western blotting detection reagents (GE Healthcare) and detected by an Ez-Capture MG imaging system (ATTO).

Measurement of conidial formation and colony radial growth rate

Conidiation of *M. oryzae* S-0412-II 2a isolate was assessed after growth of cultures on PDA or oatmeal agar (OMA) (Yang et al., 2009) at 26 °C for 14 days. Spores were harvested by flooding each culture dish with sterile distilled water and dislodging conidia with a glass rod; each plate was rinsed once with an additional aliquot of water. The spore concentration was determined by counting with a hemacytometer. To assay growth rate, *M. oryzae* was pre-cultured on a PDA plate. Mycelial disks were cut from the plate with a sterile cork borer (4 mm in diameter) and placed in the center of the a new plate, mycelial-side down. After incubation at 26 °C for 14 days, the radial growth rate was determined by measuring colony radius. Colony growth was recorded by measuring the radius of colonies in four directions at right angles and taking the mean of at least three replicates.

Curing M. oryzae S-0412-II 2a of MoCV1-B

After freezing and thawing fungal agar plugs of MoCV1-B-infected S-0412-II 2a isolate in 20% glycerol, we cultured the plugs on PDA medium at 26 °C. Some segments recovered formation of normal aerial hyphae and pigmentation. Samples from these areas were picked up and cultured to isolate single conidia. After conidial germination on PDA agar, we selected clones showing normal colony morphology. We extracted total nucleic acids from these normally growing isolates as candidates for MoCV1-B-free isolates and digested them with DNase I (TaKaRa Bio, Kyoto, Japan) and S1 nuclease (TaKaRa Bio) to investigate the presence or absence of the mycoviral dsRNAs by agarose gel electrophoresis followed by staining with 250 ng/ml ethidium bromide. RT-PCR using dsRNA1-specific primers was performed to confirm absence of the MoCV1-B dsRNA1.

Northern hybridization

dsRNA was extracted with SDS/phenol and purified by chromatography on CF-11 cellulose (Whatman, UK) from cultured mycelia as described by Morris and Dodds (1979). Samples were heat-denatured before electrophoretic separation on a 1.2% agarose, 0.66 M formaldehyde gel, transferred to a Zeta-Probe nylon membrane (Bio-Rad) and cross-linked by UV irradiation. After prehybridization in 250 mM phosphate buffer, pH 7.2, 1 mM EDTA, 7% SDS, 1% BSA, blots were hybridized for 16 h at 65 °C in the same solution with digoxigenin (DIG)-labeled DNA probes specific for MoCV1-B dsRNA5 (1945–2606 nt). Probes were synthesized with a DIG-High Prime random primer labeling kit (Roche Applied Science, Indianapolis, IN, USA). Membranes were washed twice at 65 °C with 40 mM phosphate buffer, pH 7.2, containing 5% SDS for 30 min and twice at 65 °C with 40 mM phosphate buffer, pH 7.2, containing 1% SDS for 30 min. Probes were detected using a Detection Starter Kit I (Roche) and the CDP-Star ready-to-use substrate (Roche Applied Science) according to the manufacturer's protocol. Signals were scanned with an AE-9300 Ez-Capture MG luminescent image analyzer (ATTO).

Light microscopy of M. oryzae

Mycelial plugs were inoculated into fermentation reactors (2.5 L, ABLE Biott) containing 1.5 L YG broth at 27 °C, then cultured with agitation at 100 rpm and with air introduced at 1.5 L min^{-1}. After 3 days of culture, mycelia were examined at 1000 × magnification with an IX71 light microscope (Olympus, Tokyo, Japan) and differential interference contrast optics.

Acknowledgments

This research was supported in part by a Grant-in-Aid for Linking Mechanism of Research Results to Practical Application from Japan Science and Technology Agency (No. 859100012); by a grant from the New Energy and Industrial Technology Development

Organization (No. 08C46503c) to H.M. and by a JSPS KAKENHI grant (No. 11J07853) to S.U.

Appendix A. Supporting information

Supplementary data associated with this article can be found in the online version at http://dx.doi.org/10.1016/j.virol.2013.10.022.

References

Abascal, F., Zardoya, R., Posada, D., 2005. ProtTest: selection of best-fit models of protein evolution. Bioinformatics 21, 2104–2105.

Anagnostakis, S.L., Day, P.R., 1979. Hypovirulence conversion in *Endothia parasitica*. Phytopathology 69, 1226–1229.

Aoki, N., Moriyama, H., Kodama, M., Arie, T., Teraoka, T., Fukuhara, T., 2009. A novel mycovirus associated with four double stranded RNAs affects host fungal growth in *Alternaria alternata*. Virus Res. 140, 179–187.

Bao, X., Roossinck, M.J., 2013. Multiplexed interactions: viruses of Endophytic fungi. Adv. Virus Res. (San Diego, CA, Elsevier) 86 (86), 37–57.

Bruenn, J.A., 1993. A closely related group of RNA-dependent RNA polymerases from double-stranded RNA viruses. Nucleic Acids Res. 21, 5667–5669.

Bruenn, J.A., 2002. dsRNA genetic elements. In: Tavantzis, S.M. (Ed.), Concepts and Applications in Agriculture, Forestry and Medicine. CRC Press, Boca Raton, FL, pp. 109–124.

Chiba, S., Salaipeth, L., Lin, Y.H., Sasaki, A., Kanematsu, S., Suzuki, N., 2009. A novel bipartite double-stranded RNA mycovirus from the white root rot fungus *Rosellinia necatrix*: molecular and biological characterization, taxonomic considerations, and potential for biological control. J. Virol. 83, 12801–12812.

Cho, W.K., Lee, K.M., Yu, J., Son, M., Kim, K.H., 2013. Insight into mycoviruses infecting Fusarium species. Adv. Virus Res. (San Diego, CA, Elsevier) 86 (86), 273–288.

Chu, Y.M., Jeon, J.J., Yea, S.J., Kim, Y.H., Yun, S.H., Lee, Y.W., Kim, K.H., 2002. Double stranded RNA mycovirus from Fusarium graminearum. Appl. Environ. Microbiol. 68, 2529–2534.

Darissa, O., Willingmann, P., Schafer, W., Adam, G., 2011. A novel doublestranded RNA mycovirus from Fusarium graminearum: nucleic acid sequence and genomic structure. Arch. Virol. 156, 647–658.

Dawe, A.L., Nuss, D.L., 2013. Hypovirus molecular biology: from Koch's postulates to host self-recognition genes that restrict virus transmission. Adv. Virus Res. (San Diego, CA, Elsevier) 86 (86), 109–147.

Frohman, M.A., Dush, M.K., Martin, G.R., 1988. Rapid production of full-length cDNA's from rare transcripts: amplification using a single gene specific oligonucleotide primer. Proc. Natl. Acad. Sci. USA 85, 8988–9002.

Ghabrial, S.A., 1998. Origin, adaption and evolutionary pathways of fungal viruses. Virus Genes 16, 119–131.

Ghabrial, S.A., Dunn, S.E, Li, H., Xie, J., Baker, T.S., 2013. Viruses of Helminthosporium (Cochlioblus) victoriae. Adv. Virus Res. (San Diego, CA, Elsevier) 86 (86), 289–325.

Guindon, S., Dufayard, J.F., Lefort, V., Anisimova, M., Hordijk, W., Gascuel, O., 2010. New algorithms and methods to estimate maximum-likelihood phylogenies: assessing the performance of PhyML 3.0. Syst. Biol. 59, 307–321.

Hammond, T.M., Andrewski, M.D., Roossinck, M.J., Keller, N.P., 2008. Aspergillus mycoviruses are targets and suppressors of RNA silencing. Eukaryot. Cell 7, 350–357.

Herrero, N., Zabalgogeazcoa, I., 2011. Mycoviruses infecting the endophytic and entomopathogenic fungus *Tolypocladium cylindrosporum*. Virus Res. 160, 409–413.

Hillman, B.I., Cai, G., 2013. The family narnaviridae: simplest of RNA viruses. Adv. Virus Res. (San Diego, CA. Elsevier) 86 (86), 149–176.

Jiang, D., Ghabrial, S.A., 2004. Molecular characterization of *Penicillium chrysogenum* virus: reconsideration of the taxonomy of the genus Chrysovirus. J. Gen. Virol. 85, 2111–2121.

Kanematsu, S., Arakawa, M., Oikawa, Y., Onoue, M., Osaki, H., Nakamura, H., Ikeda, K., Kuga-Uetake, Y., Nitta, H., Sasaki, A., Suzaki, K., Yoshida, K., Matsumoto, N., 2004. A reovirus causes hypovirulence of *Rosellinia necatrix*. Phytopathology 94, 561–568.

King, A.MQ., Adams, M.J., Carstens, E.B., Lefkowitz, E.J. (Eds.), 2012. Elsevier Academic Press, Amsterdam, the Netherlands.

Kondo, H., Kanematsu, S., Suzuki, N., 2013. Viruses of the white root rot fungus, Rosellinia necatrix. Adv. Virus Res. (San Diego, CA, Elsevier) 86 (86), 177–214.

Larkin, M.A., Blackshields, G., Brown, N.P., Chenna, R., McGettigan, P.A., McWilliam, H., Valentin, F., Wallace, I.M., Wilm, A., Lopez, R., Thompson, J.D., Gibson, T.J., Higgins, D.G., 2007. Clustal W and Clustal X version 2.0. Bioinformatics 23, 2947–2948.

Le, M.T., Arie, T., Teraoka, T., 2010. Population dynamics and pathogenic races of rice blast fungus, *Magnaporthe oryzae* in the Mekong Delta in Vietnam. J. Gen. Plant Pathol. 76, 177–182.

Lin, Y.H., Hisano, S., Yaegashi, H., Kanematsu, S., Suzuki, N., 2013. A second quadrivirus strain from the phytopathogenic filamentous fungus *Rosellinia necatrix*. Arch. Virol. 158, 1093–1098.

Lin, Y.H., Chiba, S., Tani, A., Kondo, H., Sasaki, A., Kanematsu, S., Suzuki, N., 2012. A novel quadripartite dsRNA virus isolated from a phytopathogenic filamentous fungus, *Rosellinia necatrix*. Virology 426, 42–50.

Li, L., Liu, J., Xu, A., Wang, T., Chena, J., Zhu, X., 2013. Molecular characterization of a trisegmented chrysovirus isolated from the radish *Raphanus sativus*. Virus Res. 176, 169–178.

Morris, T.J., Dodds, J.A., 1979. Isolation and analysis of doublestranded RNA from virus-infected plant and fungal tissue. Phytopathology 69, 854–858.

Nuss, D.L., 2005. Hypovirulence: mycoviruses at the fungal-plant interface. Nat. Rev. Microbiol. 3, 632–642.

Posada, D., Buckley, T., 2004. Model selection and model averaging in phylogenetics: advantages of akaike information criterion and bayesian approaches over likelihood ratio tests. Syst. Biol. 53, 793–808.

Tamura, K., Peterson, D., Peterson, N., Stecher, G., Nei, M., Kumar, S., 2011. MEGA5: molecular evolutionary genetics analysis using maximum likelihood, evolutionary distance, and maximum parsimony methods. Mol. Biol. Evol. 28, 2731–2739.

Thompson, J.D., Gibson, T.J., Plewniak, F., Jeanmougin, F., Higgins, D.G., 1997. The CLUSTAL X windows interface: flexible strategies for multiple sequence alignment aided by quality analysis tools. Nucleic Acids Res. 25, 4876–4882.

Urayama, S., Kato, S., Suzuki, Y., Aoki, N., Le, M.T., Arie, T., Teraoka, T., Fukuhara, T., Moriyama, H., 2010. Mycoviruses related to chrysovirus affect vegetative growth in the rice blast fungus *Magnaporthe oryzae*. J. Gen. Virol. 91, 3085–3094.

Urayama, S., Ohta, T., Onozuka, N., Sakoda, H., Fukuhara, T., Arie, T., Teraoka, T., Moriyama, H., 2012. Characterization of *Magnaporthe oryzae* chrysovirus 1 structural proteins and their expression in *Saccharomyces cerevisiae*. J. Virol. 86, 8287–8295.

Van der Lende, T.R., Duitman, E.H., Gunnewijk, M.G., Yu, L., Wessels, J.G., 1996. Functional analysis of dsRNAs (L1, L3, L5, and M2) associated with isometric 34-nm virions of Agaricus bisporus (white button mushroom). Virology 217, 88–96.

Wu, M., Jin, F., Zhang, J., Yang, L., Jiang, D., Li, G., 2012. Characterization of a novel bipartite double-stranded RNA mycovirus conferring hypovirulence in the phytopathogenic fungus Botrytis porri. J. Virol. 86, 6605–6619.

Yang, Y., Zhang, H., Li, G., Li, W., Wang, X., Song, F., 2009. Ectopic expression of MgSM1, a Cerato-platanin family protein from *Magnaporthe grisea*, confers broadspectrum disease resistance in Arabidopsis. Plant Biotechnol. J. 7, 763–777.

Yu, J., Lee, K.M., Son, M., Kim, K.H., 2011. Molecular Characterization of Fusarium Graminearum Virus 2 Isolated from *Fusarium graminearum* Strain 98-8-60. Plant Pathol. J. 27, 285–290.

Zhang, Z., Schwartz, S., Wagner, L., Miller, W., 2000. A greedy algorithm for aligning DNA sequences. J. Comput. Biol. 7, 203–214.